mobility and yield a charge of 12 ± 2 e⁻ per tubulin dimer under physiological conditions. This value may be important to elucidate the effect of in vivo electric forces on microtubules. Endogenous physiological electric fields, with a typical value up to 10^3 V/m, are shown to be involved in cell division, wound healing (*35*), and embryonic cell development (*36*), but their microscopic effect has so far not been understood. The application of biomotors in nanofabricated environments is an exciting development, offering novel possibilities for future developments in lab-on-chip sorting or purification applications.

References and Notes

1. R. K. Soong *et al.*, *Science* **290**, 1555 (2000).
2. F. Patolsky, Y. Weizmann, I. Willner, *Nat. Mater.* **3**, 692 (2004).
3. J. Xi, J. J. Schmidt, C. D. Montemagno, *Nat. Mater.* **4**, 180 (2005).
4. H. Hess, V. Vogel, *J. Biotechnol.* **82**, 67 (2001).
5. M. J. Schnitzer, S. M. Block, *Nature* **388**, 386 (1997).
6. K. J. Bohm, J. Beeg, G. M. zu Horste, R. Stracke, E. Unger, *IEEE Trans. Adv. Packag.* **28**, 571 (2005).
7. R. Yokokawa *et al.*, *Nano Lett.* **4**, 2265 (2004).
8. H. Hess, G. D. Bachand, V. Vogel, *Chemistry* **10**, 2110 (2004).
9. J. Clemmens *et al.*, *Langmuir* **19**, 10967 (2003).
10. S. G. Moorjani, L. Jia, T. N. Jackson, W. O. Hancock, *Nano Lett.* **3**, 633 (2003).
11. L. Jia, S. G. Moorjani, T. N. Jackson, W. O. Hancock, *Biomed. Microdevices* **6**, 67 (2004).
12. M. G. L. van den Heuvel, C. T. Butcher, S. G. Lemay, S. Diez, C. Dekker, *Nano Lett.* **5**, 235 (2005).
13. Y. Hiratsuka, T. Tada, K. Oiwa, T. Kanayama, T. Q. P. Uyeda, *Biophys. J.* **81**, 1555 (2001).
14. M. G. L. van den Heuvel, C. T. Butcher, R. M. M. Smeets, S. Diez, C. Dekker, *Nano Lett.* **5**, 1117 (2005).
15. S. Ramachandran, K. Ernst, G. D. Bachand, V. Vogel, H. Hess, *Small* **2**, 330 (2006).
16. R. Stracke, K. J. Bohm, L. Wollweber, J. A. Tuszynski, E. Unger, *Biochem. Biophys. Res. Commun.* **293**, 602 (2002).
17. Materials and methods are available as supporting information on *Science* Online.
18. At large fields, higher than ~110 kV/m, we observed an effect on the microtubule velocity along the electric field. Microtubules moving parallel to the electric field displayed higher and lower speeds depending on the direction of the field. For fields oriented perpendicular to the long axis, microtubules displayed sideward motion. We are investigating these effects.
19. T. Duke, T. E. Holy, S. Leibler, *Phys. Rev. Lett.* **74**, 330 (1995).
20. D. Stigter, *J. Phys. Chem.* **82**, 1417 (1978).
21. D. Stigter, C. Bustamante, *Biophys. J.* **75**, 1197 (1998).
22. The electrophoretic force on stationary microtubules in the absence of a bulk EOF consists of a direct force on the negative microtubule charge, $-|\sigma|\mathbf{E}$, and an opposing indirect friction, τ, exerted by the microtubule's counterions moving along the electric field. The velocity of the counterions increases from 0 at the microtubule surface to $|\mu_e|\mathbf{E}$. If $\lambda_D \ll R$, the magnitude of $\tau = +|\sigma|\mathbf{E} - c|\mu_e|\mathbf{E}$ and also equals the total force density exerted on the double layer, plus the drag force exerted on the moving counterions (*21*).
23. D. Stigter, *Biopolymers* **31**, 169 (1991).
24. The value of $g_\perp$ only depends on the ζ potential of a microtubule and the relative thickness of the double layer (λ_D) with respect to the cylinder radius a, i.e., $g_\perp = \Im(\zeta, a/\lambda_D)$, and numerical values have been tabulated (*20*). In the limit of infinitely small λ_D, $g_\perp$ reaches its maximum value of 1.5 and $\mu_{e,\perp} \rightarrow \mu_{e,\parallel}$. The experimentally determined value of $g_\perp$ is thus a measure of the ζ potential by $\zeta = \Im^{-1}(g_\perp, a/\lambda_D)$, using a = 12.5 nm and λ_D = 0.8 nm for the Debye length in our 160 mM buffer.
25. A. J. Hunt, F. Gittes, J. Howard, *Biophys. J.* **67**, 766 (1994).
26. We calculate $c_\perp$ using the analytical result from Hunt *et al*. (*25*) with the following numerical values: Microtubule radius a = 12.5 ± 1 nm, viscosity η = 0.89 ± 0.09 × 10^{-3} kg/ms, and h = 30 ± 10 nm for the distance of the microtubule axis to the surface.
27. F. Gittes, B. Mickey, J. Nettleton, J. Howard, *J. Cell Biol.* **120**, 923 (1993).
28. H. Felgner, R. Frank, M. Schliwa, *J. Cell Sci.* **109**, 509 (1996).
29. For long microtubules and high kinesin density, the persistence length of the microtubule trajectory L_{tr} equals the persistence length of the tip L_p (*19*). This trajectory persistence length of microtubules in the absence of electric fields has been quantified to be 0.11 mm (*37*). Our value of the tip persistence length is close to this value. The suggestion of Kis *et al.* (*38*) that protofilament sliding reduces the stiffness of short lengths of microtubules could serve as a possible explanation of the low L_p, together with possible defects in the tip structure.
30. The use of the linear Grahame equation is strictly speaking only valid for $\zeta \ll k_BT/e$ = 26 mV. However, at ζ = 50 mV, the use of the linearized Grahame equation introduces an error in σ of only 14%. The use of the nonlinear version of the Grahame would invoke an unknown source of error, because we would then have to assume a value for the double-layer capacitance of the microtubule.
31. E. Nogales, S. G. Wolf, K. H. Downing, *Nature* **393**, 191 (1998).
32. P. S. Dittrich, P. Schwille, *Anal. Chem.* **75**, 5767 (2003).
33. A. Y. Fu, C. Spence, A. Scherer, F. H. Arnold, S. R. Quake, *Nat. Biotechnol.* **17**, 1109 (1999).
34. H. A. Stone, A. D. Stroock, A. Ajdari, *Annu. Rev. Fluid Mech.* **36**, 381 (2004).
35. B. Song, M. Zhao, J. V. Forrester, C. D. McCaig, *Proc. Natl. Acad. Sci. U.S.A.* **99**, 13577 (2002).
36. K. R. Robinson, L. F. Jaffe, *Science* **187**, 70 (1975).
37. T. Nitta, H. Hess, *Nano Lett.* **5**, 1337 (2005).
38. A. Kis *et al.*, *Phys. Rev. Lett.* **89**, 248101 (2002).

39. We thank J. Howard and S. Diez for kindly providing us with the kinesin expression vector and for advice with protocols; S. G. Lemay, I. Dujovne, and D. Stein for useful discussions; Y. Garini and Olympus Netherlands for lending optical equipment; and Hamamatsu Germany for kindly providing us a C7780 color camera. This work was funded by the Dutch Organization for Scientific Research (NWO) and the European Community Biomach program.

Supporting Online Material

www.sciencemag.org/cgi/content/full/312/5775/910/DC1
Materials and Methods
SOM Text
Figs. S1 and S2
References and Notes
Movie S1

23 December 2005; accepted 9 March 2006
10.1126/science.1124258

PIN Proteins Perform a Rate-Limiting Function in Cellular Auxin Efflux

Jan Petrášek,[1,2] Jozef Mravec,[3] Rodolphe Bouchard,[4] Joshua J. Blakeslee,[5] Melinda Abas,[6] Daniela Seifertová,[1,2,3] Justyna Wiśniewska,[3,7] Zerihun Tadele,[8] Martin Kubeš,[1,2] Milada Čovanová,[1,2] Pankaj Dhonukshe,[3] Petr Skůpa,[1,2] Eva Benková,[3] Lucie Perry,[1] Pavel Křeček,[1,2] Ok Ran Lee,[5] Gerald R. Fink,[9] Markus Geisler,[4] Angus S. Murphy,[5] Christian Luschnig,[6] Eva Zažímalová,[1]* Jiří Friml[3,10]

Intercellular flow of the phytohormone auxin underpins multiple developmental processes in plants. Plant-specific pin-formed (PIN) proteins and several phosphoglycoprotein (PGP) transporters are crucial factors in auxin transport–related development, yet the molecular function of PINs remains unknown. Here, we show that PINs mediate auxin efflux from mammalian and yeast cells without needing additional plant-specific factors. Conditional gain-of-function alleles and quantitative measurements of auxin accumulation in *Arabidopsis* and tobacco cultured cells revealed that the action of PINs in auxin efflux is distinct from PGP, rate-limiting, specific to auxins, and sensitive to auxin transport inhibitors. This suggests a direct involvement of PINs in catalyzing cellular auxin efflux.

Auxin, a regulatory compound, plays a major role in the spatial and temporal coordination of plant development (*1*–*3*). The directional active cell-to-cell transport controls asymmetric auxin distribution, which underlies multiple patterning and differential growth processes (*4*–*7*). Genetic approaches in *Arabidopsis thaliana* identified candidate genes coding for regulators of auxin transport, among them permease-like AUX1 (*8*), plant-specific PIN proteins (*9*) (fig. S1), and homologs of human multiple drug resistance transporters PGP1 and PGP19 (*10*, *11*). PGP1 has been shown to mediate the efflux of auxin from *Arabidopsis* protoplasts and heterologous systems such as yeast and HeLa cells (*12*). Similarly, PIN2 in yeast conferred decreased retention of structural auxin analogs (*13*, *14*). Plants defective in PIN function show altered auxin distribution and diverse developmental defects, all of which can be phenocopied by chemical inhibition of auxin efflux (*1*, *4*–*7*, *9*). All results demonstrate that PINs are essential components of the auxin transport machinery, but the exact mechanism of their action remains unclear.

Studies of the molecular function of PINs have been hampered mainly by the technical inability to quantitatively assess auxin flow across the plasma membrane (PM) in a multicellular system. We therefore established *Arabidopsis* cell suspension culture from the *XVE-PIN1* line, in which we placed the *PIN1* sequence under control of the estradiol-inducible promoter (*15*). Treatment with estradiol led to the activation of *PIN1* expression as shown by the coexpressed green fluorescent protein (GFP) reporter and reverse transcription polymerase chain reaction (RT-PCR) of *PIN1* in seedlings (Fig. 1A) and cultured cells (fig. S2). In estradiol-treated *XVE-PIN1* cells, the overexpressed PIN1 was localized at the PM (Fig. 1, B and C). The syn-

thetic auxin naphthalene-1-acetic acid (NAA) enters cells easily by diffusion and is a poor substrate for active uptake but an excellent substrate for active efflux (*16*). Therefore, change in accumulation of radioactively labeled NAA inside cells provides a measure of the rate of auxin efflux from cells. Untreated *XVE-PIN1* cells as well as nontransformed cells displayed [^{3}H]NAA accumulation kinetics indicative of saturable auxin efflux and sensitive to a well-established (*1*, *9*) noncompetitive inhibitor of auxin efflux: 1-naphthylphthalamic acid (NPA) (Fig. 1D). Estradiol did not influence control cells but led to substantial decrease of [^{3}H]NAA accumulation in *XVE-PIN1* cells (Fig. 1, D and E). This demonstrates that PIN1 overexpression leads to the stimulation of efflux of auxin from *Arabidopsis* cultured cells.

Arabidopsis cultured cells are not sufficiently friable to be useful in transport assays. Instead, we used tobacco BY-2 cells, a well-established model for quantitative studies of cellular auxin transport (*17*). PIN7, the most representative member of the subfamily including *PIN1*, *PIN2*, *PIN3*, *PIN4*, *PIN6*, and *PIN7* (fig. S1), was placed under the control of a dexamethasone (DEX)–inducible system (*18*) and stably transformed into BY-2 cells. The resulting line (*GVG-PIN7*) showed up-regulation of *PIN7* expression as early as 2 hours after DEX treatment and the up-regulated PIN7 protein was detected at the PM (Fig. 2A). Nontransformed cells displayed saturable, NPA-sensitive [^{3}H]NAA efflux, which was unaffected by DEX (Fig. 2B). Induction of expression of PIN7 or its close (PIN4) and the most distant (PIN6) homologs (fig. S1) resulted in a decrease in [^{3}H]NAA accumulation, to roughly half of the original level (Fig. 2C). The kinetics of NAA efflux after the initial loading of BY-2 cells (Fig. 2D), as well as displacement curves using competitive inhibition by nonlabeled NAA (fig. S3A), clearly confirm that PIN7 overexpression stimulates saturable efflux of auxin from cells. The efflux of other auxins—such as synthetic 2,4-dichlorophenoxyacetic acid (2,4-D) or naturally occurring indole-3-acetic acid (IAA), but not its precursor tryptophan—was also stimulated (Fig. 2, E and G). The PIN7-dependent efflux of all auxins was NPA sensitive (Fig. 2G), competitively inhibited by nonlabeled NAA, and unaffected by the structurally related but biologically inactive weak organic acid, benzoic acid (BeA) (fig. S3B). Furthermore, the increasing levels of induced PIN7, as achieved with the use of different concentrations of DEX for induction, and monitored by dot blot, clearly correlated with the gradual increase in [^{3}H]NAA efflux (Fig. 2F). These data imply that different PIN proteins are rate-limiting factors in NPA-sensitive, saturable efflux of auxins from BY-2 cells. This similarity in the molecular function of PINs, together with the diversity in their regulation, provides a basis for their complex functional redundancy observed in planta (*6*, *19*, *20*).

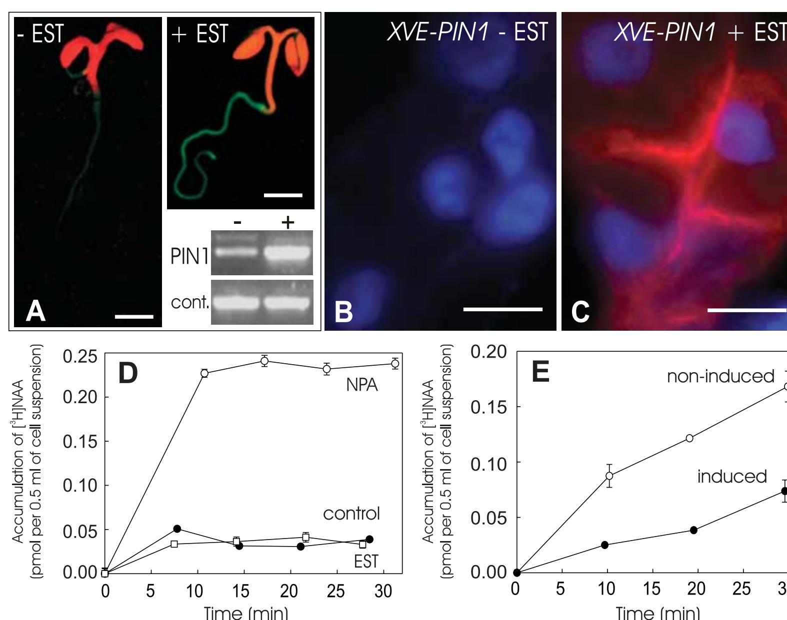

Fig. 1. PIN1-dependent auxin efflux in *Arabidopsis* cultured cells. (**A**) Up-regulation of PIN1 expression in *XVE-PIN1 Arabidopsis* seedlings after estradiol (EST) treatment (1 μM, 4 hours). The expression of coupled GFP reporter (green) and RT-PCR of *PIN1* [PGP19 expression was used as a control (cont.)] are shown. Scale bars, 3 mm. (**B** and **C**) Anti-PIN1 immunostaining (red) at the PM of *XVE-PIN1* cultured cells after EST treatment (1 μM, 24 hours) (C). There was no signal in the untreated control (B). Nuclear counterstain is shown in blue. Scale bars, 10 μm. (**D**) Auxin accumulation in *Arabidopsis* wild-type cells. NPA (10 μM) increased [^{3}H]NAA accumulation inside cells, demonstrating inhibition of auxin efflux. EST treatment (1 μM, 24 hours) had no effect on [^{3}H]NAA accumulation. (**E**) [^{3}H]NAA accumulation kinetics in *XVE-PIN1* cells, demonstrating PIN1-dependent stimulation of NAA efflux after PIN1 overexpression. Error bars show SEM (n = 4); where error bars are not shown, the error was smaller than the symbols.

The evidence from cultured cells shows that PIN proteins are key rate-limiting factors in cellular auxin efflux. This approach, however, cannot distinguish whether PINs play a catalytic role in auxin efflux or act as positive regulators of endogenous plant auxin efflux catalysts. To address this issue, we used a nonplant system: Human HeLa cells contain neither PIN-related genes nor auxin-related machinery and allow efficient heterologous expression of functional eukaryotic PM proteins (*21*). We transfected HeLa cells with *PIN7* and its more distant homolog *PIN2*. Transfected cells showed strong PIN expression (Fig. 3A), which resulted in a substantial stimulation of net efflux of natural auxin [^{3}H]IAA, compared with empty vector controls (Student's t test: $P < 0.001$) (Fig. 3B). Efflux of [^{3}H]BeA was also stimulated but to a lesser extent. These data show that PIN proteins are capable of stimulating cellular auxin efflux in the heterologous HeLa cell system, albeit with decreased substrate specificity.

To test the role of PIN proteins in another evolutionarily distant nonplant system, we used yeast (*Saccharomyces cerevisiae*). PIN2 and PIN7 were expressed in yeast and showed localization at the PM (Fig. 3A). Kinetics of relative [^{3}H]IAA retention demonstrated that expression of the PINs led to a substantial increase in IAA efflux (Fig. 3C). Efflux assays in conjunction with control experiments, including testing metabolically less active yeast in the stationary phase, or after glucose starvation (Fig. 3D), confirmed an active PIN-dependent export of IAA and, to a lesser extent, of BeA from yeast (Fig. 3C and fig. S4B). To test the requirements of the subcellular localization for PIN2 action in yeast, we performed a mutagenesis of the PIN2 sequence to isolate mistargeted mutants. One of the mutations, which changed serine-97 to glycine (pin2Gly97), led to the localization of pin2Gly97

[1]Institute of Experimental Botany, the Academy of Sciences of the Czech Republic, 165 02 Prague 6, Czech Republic. [2]Department of Plant Physiology, Faculty of Science, Charles University, 128 44 Prague 2, Czech Republic. [3]Center for Plant Molecular Biology (ZMBP), University Tübingen, D-72076 Tübingen, Germany. [4]Zurich-Basel Plant Science Center, University of Zurich, Institute of Plant Biology, CH 8007 Zurich, Switzerland. [5]Department of Horticulture, Purdue University, West Lafayette, IN 47907, USA. [6]Institute for Applied Genetics and Cell Biology, University of Natural Resources and Applied Life Sciences–Universität für Bodenkultur, A-1190 Wien, Austria. [7]Department of Biotechnology, Institute of General and Molecular Biology, 87-100 Toruń, Poland. [8]Institute of Plant Sciences, University of Bern, 3013 Bern, Switzerland. [9]Whitehead Institute for Biomedical Research, Nine Cambridge Center, Cambridge, MA 02142, USA. [10]Masaryk University, Department of Functional Genomics and Proteomics, Laboratory of Molecular Plant Physiology, Kamenice 5, 625 00 Brno, Czech Republic.

*To whom correspondence should be addressed. E-mail: eva.zazim@ueb.cas.cz

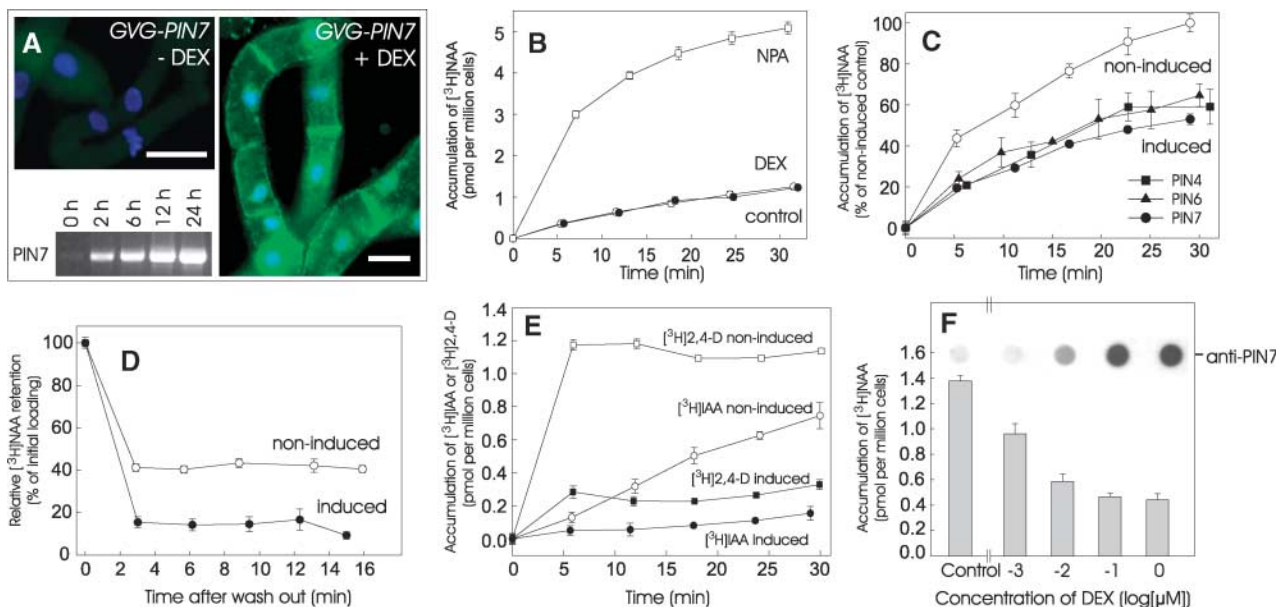

Fig. 2. PIN-dependent auxin efflux in BY-2 tobacco cultured cells. (**A**) Inducible PIN7 expression in *GVG-PIN7* tobacco cells. PIN7 immunostaining (green) is shown at the PM after DEX treatment (24 hours; 1 μM) but not in the untreated control; RT-PCR of *PIN7* was conducted within 24 hours of DEX treatment (1 μM). Nuclear counterstain is shown in blue. Scale bars, 40 μm. (**B**) Auxin accumulation in BY-2 control cells. NPA (10 μM) increased [^{3}H]NAA accumulation inside cells, demonstrating inhibition of auxin efflux. DEX treatment (1 μM, 24 hours) had no effect on [^{3}H]NAA accumulation. (**C**) [^{3}H]NAA accumulation kinetics in *GVG-PIN4*, *GVG-PIN6*, and *GVG-PIN7* cells demonstrating PIN4-, PIN6-, and PIN7-dependent stimulation of NAA efflux. Noninduced control is shown only for PIN7; those for PIN4 and PIN6 were within the range ±8% of the values for PIN7. Data are expressed as a percentage of noninduced control at 30 min after application of labeled [^{3}H]NAA. (**D**) Induced *GVG-PIN7* cells showed decreased retention of [^{3}H]NAA compared with noninduced control. (**E**) Accumulation kinetics in induced *GVG-PIN7* cells revealed PIN7-dependent stimulation of [^{3}H]IAA and [^{3}H]2,4-D efflux. (**F**) Treatments with increasing concentrations of DEX led to gradually higher levels of PIN7 in *GVG-PIN7* cells, as determined by dot blot (top) and to concomitant decrease of [^{3}H]NAA accumulation. (**G**) NPA inhibition of both endogenous and PIN7-dependent efflux of [^{3}H]NAA, [^{3}H]2,4-D, and [^{3}H]IAA. PIN7 overexpression or NPA treatment did not affect accumulation of related compound, [^{3}H]Trp. Open bars, noninduced cells; gray bars, induced cells. For all experiments, error bars show SEM (n = 4); where error bars are not shown, the error was smaller than the symbols.

in intracellular compartments (Fig. 3A). When tested in the [^{3}H]IAA efflux assay (fig. S4A), pin2Gly97 failed to mediate auxin efflux but rather increased [^{3}H]IAA accumulation inside cells (Fig. 3D). This shows that pin2Gly97 is still functional but fails to mediate auxin efflux, suggesting importance of PIN localization at PM. Overall, the results suggest that in yeast as well, PM-localized PIN proteins mediate, although with decreased specificity, a saturable efflux of auxin.

A role in auxin efflux has also been reported recently for PGP1 and, in particular, PGP19 proteins of *Arabidopsis* (*12*). PIN and PGP proteins seem to have a comparable effect on mediating auxin efflux in yeast and HeLa cells, but the genetic interference with their function in *Arabidopsis* has distinctive effects on development. All aspects of the *pin* mutant phenotypes can be mimicked by chemical interference with auxin transport (*4*–*7*, *9*). In contrast, *pgp1*/*pgp19* double mutants show strong but entirely different defects (*10*, *11*), which cannot be phenocopied by auxin transport inhibitors.

To compare the roles of PINs and PGPs in auxin efflux, we constructed the *GVG-PGP19:HA* (hemagglutinin) cell line of BY-2. DEX treatment led to the up-regulation of PGP19:HA protein, which was detected at the PM (Fig. 4A), and to a decrease in [^{3}H]NAA accumulation, similar to that observed in the *GVG-PIN4*, *GVG-PIN6*, and *GVG-PIN7* lines (Fig. 4B, compare with Fig. 2C). BeA did not interfere with [^{3}H]NAA accumulation and [^{3}H]Trp accumulation did not change after DEX treatment. However, compared with PIN-mediated auxin efflux, the PGP19-mediated NAA efflux was notably less sensitive to NPA. Whereas PIN-mediated transport was completely inhibited by NPA, about 20% of PGP19-dependent transport was NPA insensitive (Fig. 4C).

To address whether PIN action in planta requires PGP1 and PGP19 proteins, we analyzed effects of PIN1 overexpression on plant development in *pgp1*/*pgp19* double mutants. PIN1 overexpression in *XVE-PIN1* led to pronounced defects in root gravitropism, which could be detected within 4 hours after estradiol treatment. Quantitative evaluation of reorientation of root growth revealed that PIN1 overexpression in *pgp1*/*pgp19* had the same effects (Fig. 4D). These data show that PIN1 action on plant development does not strictly require function of PGP1 and PGP19 proteins, and they suggest that PINs and PGPs molecularly characterize distinct auxin transport systems. This is also supported by evidence that PIN2 mediates auxin efflux in yeast, which is known to lack homologs to *Arabidopsis* PGP proteins (*21*). It is still unclear whether these two auxin transport machineries act in planta entirely independently or in a coordinated fashion.

Rate-limiting, saturable, and specific action of PIN proteins in mediating auxin movement

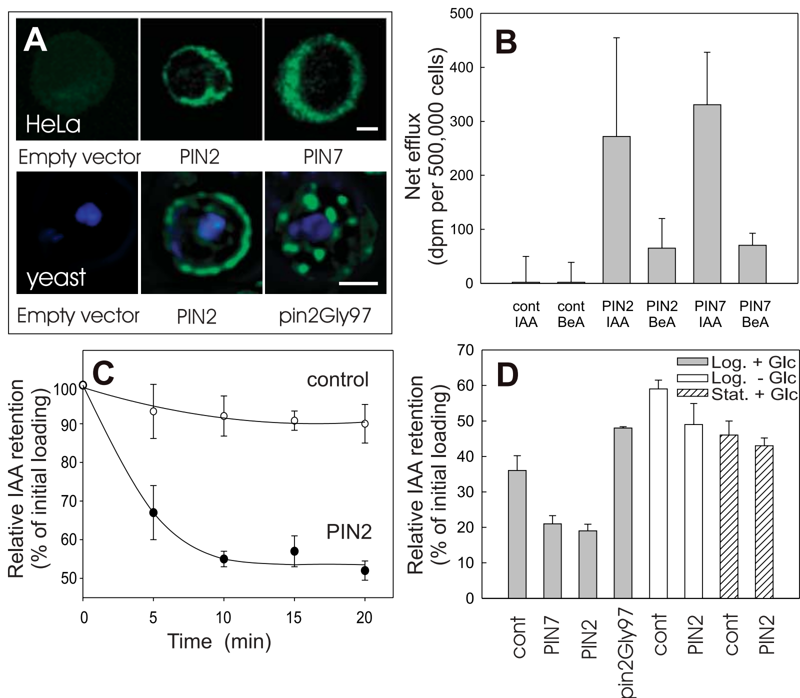

Fig. 3. PIN-dependent auxin efflux in mammalian and yeast cells. (**A**) PIN2:HA and PIN7:HA expression in HeLa and yeast. Anti-HA immunostaining detected PIN2:HA and PIN7:HA at the PM of transfected but not control (empty vector) HeLa cells (top). Anti-PIN2 immunostaining detected PIN2 at the PM and pin2Gly97 in intracellular compartments, compared with empty vector controls (bottom). Scale bars, 2 μm. (**B**) Transfected HeLa cells display PIN2- and PIN7-dependent net efflux of [^{3}H]IAA and to a smaller extent also of [^{3}H]BeA. dpm, disintegration per minute. (**C**) The kinetics of [^{3}H]IAA efflux. PIN2 stimulated saturable [^{3}H]IAA efflux in yeast JK93da strain. (**D**) [^{3}H]IAA retention measured 10 min after loading: PIN2 and PIN7 mediated [^{3}H]IAA efflux; pin2Gly97 failed to mediate efflux but increased [^{3}H]IAA retention. Yeast in stationary phase or without glucose showed much less [^{3}H]IAA efflux. Error bars show SEM (n = 4).

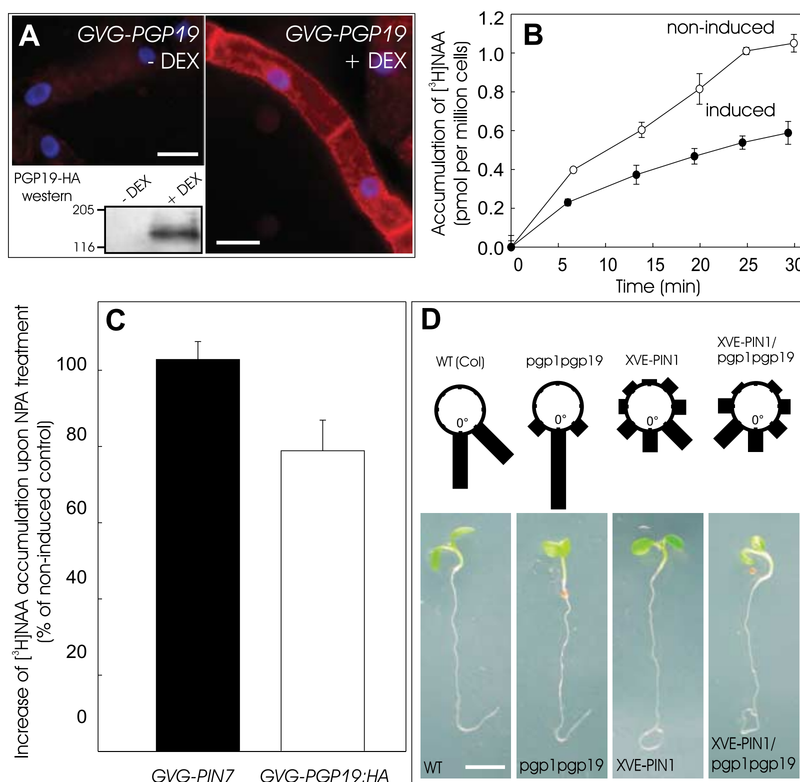

Fig. 4. Requirement of PGP function for PIN role in auxin efflux. (**A**) Inducible PGP19 expression in *GVG-PGP19:HA* tobacco cells. PGP19:HA immunostaining (red) at PM after DEX treatment (24 hours, 1 μM) is shown; no PGP19:HA immunostaining was present in the untreated control. An anti-HA immunoblot was conducted after 24 hours of DEX (1 μM) treatment. Nuclear counterstain is shown in blue. Scale bars, 40 μm. (**B**) [^{3}H]NAA accumulation decreased upon PGP19 expression, revealing function in auxin efflux in BY-2 cells. (**C**) Different sensitivities of PIN7- and PGP19-dependent [^{3}H]NAA efflux to NPA treatment (10 μM, 20 min) in *GVG-PIN7* and *GVG-PGP19:HA* cells (*23*). (**D**) Root gravitropism in *XVE-PIN1* seedlings. PIN1 overexpression (4 hours, 4 μM EST) led to gravitropic defects in *pgp1/pgp19* mutants in contrast to gravitropic growth of EST-treated nontransformed wild-type (WT) and *pgp1/pgp19* seedlings. Root gravitropism was scored 12 hours after gravity stimulation (n > 40). Scale bar, 3 mm. For (B) and (C), error bars show SEM (n = 4); where error bars are not shown, the error was smaller than the symbols.

across the PM out of plant cells largely clarifies a role of PIN proteins in intercellular auxin transport. Furthermore, the polar, subcellular PIN localization provides a vectorial component to the directional auxin flow (*22*). Therefore, transport function of PINs together with their asymmetric subcellular localization defines directional local auxin distribution underlying different developmental processes.

References and Notes

1. J. Friml, *Curr. Opin. Plant Biol.* **6**, 7 (2003).
2. A. W. Woodward, B. Bartel, *Ann. Bot. (Lond.)* **95**, 707 (2005).
3. S. Kepinski, O. Leyser, *Curr. Biol.* **15**, R208 (2005).
4. J. Friml, J. Wisniewska, E. Benková, K. Mendgen, K. Palme, *Nature* **415**, 806 (2002).
5. J. Friml *et al.*, *Cell* **108**, 661 (2002).
6. J. Friml *et al.*, *Nature* **426**, 147 (2003).
7. E. Benková *et al.*, *Cell* **115**, 591 (2003).
8. M. Bennett *et al.*, *Science* **273**, 948 (1996).
9. I. A. Paponov, W. D. Teale, M. Trebar, I. Blilou, K. Palme, *Trends Plant Sci.* **10**, 170 (2005).
10. B. Noh, A. S. Murphy, E. P. Spalding, *Plant Cell* **13**, 2441 (2001).
11. J. J. Blakeslee, W. A. Peer, A. S. Murphy, *Curr. Opin. Plant Biol.* **8**, 494 (2005).
12. M. Geisler *et al.*, *Plant J.* **44**, 179 (2005).
13. R. Chen, *Proc. Natl. Acad. Sci. U.S.A.* **95**, 15112 (1998).
14. C. Luschnig, R. A. Gaxiola, P. Grisafi, G. R. Fink, *Genes Dev.* **12**, 2175 (1998).

15. J. Zuo, Q. W. Niu, N. H. Chua, *Plant J.* **24**, 265 (2000).
16. A. Delbarre, P. Muller, V. Imhoff, J. Guern, *Planta* **198**, 532 (1996).
17. J. Petrášek *et al.*, *Plant Physiol.* **131**, 254 (2003).
18. T. Aoyama, N. H. Chua, *Plant J.* **11**, 605 (1997).
19. I. Blilou, *Nature* **433**, 39 (2005).
20. A. Vieten *et al.*, *Development* **132**, 4521 (2005).
21. M. Geisler, A. S. Murphy, *FEBS Lett.* **580**, 1094 (2006).
22. J. Wiśniewska, *Science* **312**, 883 (2006).
23. Materials and methods are available as supporting material on *Science* Online.

24. We thank N. H. Chua for providing material, V. Croy for help with HeLa studies, and P. Brewer and M. Sauer for critical reading of the manuscript. This work was supported by the European Molecular Biology Organization Young Investigator programme (J.F.), the Volkswagenstiftung (J.F., J.M., D.S., P.D.), the Grant Agency of the Academy of Sciences of the Czech Republic, project A6038303 (E.Z., M.Č., M.K., P.K., J.P., L.P., D.S., and P.S.), the Ministry of Education of the Czech Republic, projects MSM0021622415 and LC06034, the Alexander von Humboldt Foundation (Feodor Lynen fellowship to M.G.), the Foundation for Polish Science (J.W.), Margarete von Wrangell-Habilitationsprogramm (E.B.), NSF grant 0132803 (A.M., J.B., and O.L.), and Austrian Science Fund (FWF) grant 16311 (L.A. and C.L).

Supporting Online Material
www.sciencemag.org/cgi/content/full/1123542/DC1
Materials and Methods
Figs. S1 to S4
References

7 December 2005; accepted 14 March 2006
Published online 6 April 2006;
10.1126/science.1123542
Include this information when citing this paper.

Oceanographic Basis of the Global Surface Distribution of *Prochlorococcus* Ecotypes

Heather A. Bouman,[1]* Osvaldo Ulloa,[1] David J. Scanlan,[3] Katrin Zwirglmaier,[3] William K. W. Li,[4] Trevor Platt,[4] Venetia Stuart,[5] Ray Barlow,[6] Ole Leth,[2] Lesley Clementson,[7] Vivian Lutz,[8] Masao Fukasawa,[9] Shuichi Watanabe,[9] Shubha Sathyendranath[5]

By using data collected during a continuous circumnavigation of the Southern Hemisphere, we observed clear patterns in the population-genetic structure of *Prochlorococcus*, the most abundant photosynthetic organism on Earth, between and within the three Southern Subtropical Gyres. The same mechanisms that were previously invoked to account for the vertical distribution of ecotypes at local scales accounted for the global (horizontal) patterns we observed. Basin-scale and seasonal variations in the structure and strength of vertical stratification provide a basis for understanding large-scale horizontal distribution in genetic and physiological traits of *Prochlorococcus*, and perhaps of marine microbial communities in general.

Prochlorococcus is the smallest and most abundant phytoplankter in the global ocean and contributes significantly to the primary productivity of tropical and subtropical oceans (*1*). That the genus thrives throughout a wide range of photic zone conditions has been explained by the discovery of genetically and physiologically distinct populations, commonly referred to as high light (HL)– and low light (LL)–adapted ecotypes (*2*). *Prochlorococcus* ecotypes partition themselves according to depth in a stratified water column (*3*); however, the coexistence of multiple ecotypes (*2*) and phylotypes (*4*–*6*) has also been reported and attributed to vertical mixing in response to local physical forcing. But the effect of physical forcing on *Prochlorococcus* ecotypes at the global scale has not been explored. By using data collected during a circumnavigation of the Southern Hemisphere, we investigated whether the genetic structure of *Prochlorococcus* populations changes in response to vertical mixing within and between the major ocean basins of the world.

Samples were collected during the Blue Earth Global Expedition (BEAGLE) (Fig. 1A). The 7-month expedition spanned the southern Pacific (winter), Atlantic (late spring), and Indian (summer) Oceans (*7*); covered several biogeochemical provinces (*8*); and provided a rare opportunity to study physical forcing of phytoplankton at the global scale. We used the depth of the surface mixed layer (z_m) and the strength of the vertical density gradient (N) as indicators of the physical state of the water column (*9*). The three ocean basins differed markedly in these properties (Fig. 1B). The basin-scale variations in the vertical structure of the water column observed in the BEAGLE data are partly due to seasonal and latitudinal differences in the sampling of the three ocean basins. Mixed-layer–depth climatology reveals strong seasonality in z_m, with high values of z_m occurring during the Austral winter in all three ocean basins, and relatively uniform and shallow z_m values in the summer months (fig. S1). However, differences among basins are also found. Thus, spatial differences in vertical mixing as indexed by z_m observed during the BEAGLE have a seasonal as well as a geographical component.

Prochlorococcus cell abundance was determined by flow cytometry, and the concentration of divinyl chlorophyll a (DV Chla), a pigment marker for this genus, was measured by high performance liquid chromatography (HPLC). A clear difference between the geographic patterns of these two indices of abundance was found (Fig. 2A). *Prochlorococcus* abundance has a minimum in the well-mixed, mesotrophic waters of the Western Pacific Basin and a maximum in the strongly stratified oligotrophic waters of the Indian Ocean, a pattern that is consistent with our current understanding of the distribution of this genus (*1*, *10*, *11*). However, the concentration of divinyl chlorophyll a is high in the Pacific Basin (except near 140°W) and low in the Atlantic and Indian Basins. This is perhaps counterintuitive; it can be explained as follows. Because all samples were collected within the top 10 m of the water column, vertical mixing would be an important mechanism altering the growth conditions (light and nutrients) of the phytoplankton cells. Thus, the high divinyl chlorophyll a concentrations in the Pacific may arise from photoacclimatory (physiological) or photoadaptive (genetic) response of the cells to a decrease in mean light intensity. Basin-scale patterns in the intracellular concentration of divinyl chlorophyll a (C_i) for *Prochlorococcus* are evident (Fig. 2B), with low C_i values observed in the strongly stratified Indian Ocean during the summer (averaging 0.14 fg DV Chla per cell), consistent with those found in the surface waters of the subtropical North Atlantic (*12*), and high values observed in the well-mixed Archipelagic Deep Basins Province (*8*) during the winter (averaging 1.00 fg DV Chla per cell), similar to those typically found deeper in the water column in subtropical gyres (*12*).

Because light decreases exponentially with depth, phytoplankton cells mixed deeper in the water column would experience a lower mean daily irradiance than if they remained at the sea surface. Phytoplankton respond to this reduction in irradiance by increasing the concentration of pigment per cell. An inverse relation between C_i

[1]Laboratorio de Procesos Oceanográficos y Clima, Departamento de Oceanografía, and Centro de Investigación Oceanográfica en el Pacífico Sur-Oriental, [2]Departamento de Geofísica, Universidad de Concepción, Casilla 160-C, Concepción, Chile. [3]Department of Biological Sciences, University of Warwick, Coventry CV4 7AL, UK. [4]Bedford Institute of Oceanography, Dartmouth, Nova Scotia, B2Y 4A2, Canada. [5]Department of Oceanography, Dalhousie University, Halifax, Nova Scotia, B3H 4J1, Canada. [6]Marine and Coastal Management, Private Bag X2, Rogge Bay 8012, Cape Town, South Africa. [7]Commonwealth Scientific and Industrial Research Organization, Marine Research, Post Office Box 1538, Hobart, Tasmania, Australia, 7001. [8]Instituto Nacional de Investigación y Desarrollo Pesquero, Paseo Victoria Ocampo 1, 7600 Mar del Plata, Argentina. [9]Japan Agency for Marine-Earth Science and Technology, 2-15, Natsushima, Yokosuka, 237-0061, Japan.

*To whom correspondence should be addressed. E-mail: heather@profc.udec.cl

www.sciencemag.org/cgi/content/full/1123542/DC1

Supporting Online Material for

PIN Proteins Perform a Rate-Limiting Function in Cellular Auxin Efflux

Jan Petrášek, Jozef Mravec, Rodolphe Bouchard, Joshua J. Blakeslee, Melinda Abas, Daniela Seifertová, Justyna Wiśniewska, Zerihun Tadele, Martin Kubeš, Milada Čovanová, Pankaj Dhonukshe, Petr Skůpa, Eva Benková, Lucie Perry, Pavel Křeček, Ok Ran Lee, Gerald R. Fink, Markus Geisler, Angus S. Murphy, Christian Luschnig, Eva Zažímalová,* Jiří Friml

*To whom correspondence should be addressed. E-mail: eva.zazim@ueb.cas.cz

Published 6 April 2006 on *Science* Express
DOI: 10.1126/science.1123542

This PDF file includes:

Materials and Methods
Figs. S1 to S4
References

Supporting online material

Materials and Methods

Plant material, gene constructs, transformation and inducible expression

Arabidopsis seedlings were grown at a 16 hours light/8 hours dark cycle at 18-25 °C on 0.5 x MS with sucrose as described (*1*). The *XVE-PIN1* (Col-0) transgenic plants were obtained by introducing the p_{G10-90}*::XVE* activator and the *LexA::PIN1*; *LexA::GFP* reporter constructs (*2, 3*) into *pin1-7* mutant line. This line was crossed with *pgp1pgp19* double mutant (*4*) to generate *XVE-PIN1/pgp1pgp19* line. The *XVE-PIN1* construct was generated using *PIN1* cDNA (GenBank accession number AF089084). *GVG-PIN4,6,7* constructs were generated by inserting the corresponding cDNAs (*PIN4*: AF087016, *PIN6*: AF087819, *PIN7*: AF087820) into the pTA7002 vector (*5*). *GVG-PGP19:HA* construct was generated by introducing the full length genomic fragment of *PGP19* (locus name At3g28860) with C-terminal hemaglutinin tag (HA) into pTA7002 vector (*5*).

Cell suspension from *XVE-PIN1 Arabidopsis* line was established from calli induced on young leaves (*6*) and grown in liquid MS medium containing 1 μM 2,4-D. BY-2 tobacco cells (*Nicotiana tabacum* L., cv. Bright Yellow 2, (*7*)) were grown as described (*8*) and stably transformed by co-cultivation with *Agrobacterium* (*8*). Transgenic tobacco cells and calli were maintained on the media supplemented with 40 μg ml^{-1} hygromycin and 100 μg ml^{-1} cefotaxim. Expression of *PIN* and *PGP* genes in tobacco cells was induced by the addition of dexamethasone (DEX, 1 μM, 24 hours, except for stated otherwise) at the

beginning of the subcultivation period. The same approach was used for *Arabidopsis* cell culture, where 1 μM β-Estradiol (EST) was added. Both DEX and EST were added from stock solutions in DMSO (200 μM), appropriate volume of DMSO was added in controls.

Expression and localization analysis

Tobacco and *Arabidopsis* RNA was isolated using the Plant RNA Qiagen Mini-Prep and RT-PCR performed using Qiagen® OneStep RT-PCR or Invitrogen SuperSriptII kits according to the manufacturer's protocols.

Total protein fraction from *GVG-PGP19* tobacco cells was obtained after homogenization in liquid nitrogen using mortar and pestle. The frozen powder was then mixed with an equal volume of extraction buffer (50 mM Tris-HCl, pH 6.8; 2 % SDS; 36 % w/v urea; 30 % v/v glycerol; 5 % v/v mercaptoethanol; 0,5 % w/v Bromphenol Blue), vortexed for 1 min, boiled for 3 min, and centrifuged at 13,000 rpm and 4°C for 5 min. The supernatant was transferred into a new tube and re-centrifuged at 13,000 rpm and 4°C for 5 min. The resulting supernatant was defined as total protein extract and stored at –20°C until use.

Microsomal protein fraction from *GVG-PIN7* tobacco cells was used for immunoblot analysis of PIN7 protein. Briefly, cells were homogenized by sonication in extraction buffer (50mM Tris pH 6.8; 5% (v/v) glycerol; 1.5% (w/v) insoluble polyvinylpolypyrrolidone; 150mM KCl; 5mM Na EDTA; 5mM Na EGTA; 50mM NaF; 20mM beta-glycerol phosphate; 0.5% (v/v) solubilized casein, 1mM benzamidine; 1mM PMSF; 1μg/ml pepstatin; 1μg/ml leupeptin; 1μg/ml aprotinin; 1 Roche Complete Mini Protease Inhibitor tablet per 10ml). After centrifugation at 3,800 x *g* for 20 minutes, the supernatant was filtered through nylon mesh and spun again at 3,800 x *g*. The supernatant was centrifuged

at 100,000 x *g* for 90 min. The resulting pellet was homogenized and re-suspended in buffer containing 50mM Tris pH 7.5; 20% glycerol; 2mM EGTA; 2mM EDTA; 50-500µM DTE; 10µg/ml solubilized casein and protease inhibitors as in the extraction buffer. Equal amounts of protein (about 10µg) were heated at 60°C for 40 min in sample buffer (3% (w/v) SDS; 40mM DTE; 180mM Tris pH 6.8; 8M urea), and transferred on PVDF membrane using dot-blot (SCIE-PLAS, U.K.) or semi-dry electro-blot. Primary rabbit polyclonal anti-PIN7 antibody (*10*) or mouse monoclonal anti-HA antibody (Sigma) followed by secondary HRP-conjugated anti-rabbit antibody and ECL detection kit (Amersham Biosciences, U.K.) were used for dot or western blot analysis.

Indirect immunofluorescence method was used for immunolocalizations in *Arabidopsis* cell suspension (11) and BY-2 cells (*8*). Briefly, *Arabidopsis* cells were fixed for 30 min at room temperature with 4% (w/v) paraformaldehyde in 0.1 M PIPES, pH 6.8, 5 mM EGTA, 2 mM $MgCl_2$, and 0.4% (w/v) Triton X-100. Cells were then treated with the solution of 0.8% (w/v) macerozyme R-10 and 0.2% (w/v) pectolyase Y-23 in 0.4 M mannitol, 5 mM EGTA, 15 mM MES, pH 5.0, 1 mM PMSF, 10 µg/ml of leupeptin, and 10 µg/ml of pepstatin A. Then the cells were washed in PBS buffer and attached to poly-L-lysine coated coverslips and incubated for 30 min in 1% (w/v) BSA in PBS and incubated for 1 h with primary antibody. The specimens were then washed three times for 10 min in PBS and incubated for 1 h with secondary antibody. Coverslips with cells were carefully washed in PBS, rinsed with water with Hoechst 33258 (0,1µg/ml) and embedded in Mowiol (Polysciences) solution.

Tobacco BY-2 cells were pre-fixed 30 min in 100 µM MBS and 30 min in 3.7% (w/v) PFA in buffer consisting of 50 mM PIPES, 2 mM EGTA, 2 mM $MgSO_4$, pH 6.9, at 25°C and

subsequently in 3.7% (w/v) PFA and 1% Triton X-100 (w/v) in stabilizing buffer for 20 minutes. After treatment with an enzyme solution (1% (w/v) macerozyme and 0.2% (w/v) pectinase) for 7 min at 25°C and 20 minutes in ice cold methanol (at -20°C), the cells were attached to poly-L-lysine coated coverslips and treated with 1% (w/v) Triton X-100 in microtubule stabilizing buffer for 20 minutes. Then the cells were treated with 0.5% (w/v) bovine serum albumin in PBS and incubated with primary antibody for 45 minutes at 25°C. After washing with PBS, a secondary antibody in PBS was applied for 1 h at 25°C. Coverslips with cells were carefully washed in PBS, rinsed with water with Hoechst 33258 (0,1μg/ml) and embedded in Mowiol (Polysciences) solution.

The following antibodies and dilutions were used: anti- PIN1 (*13*, 1: 500), anti-PIN7 (*10*, 1:500), anti-HA (Sigma-Aldrich; 1:500), TRITC- (Sigma-Aldrich; 1:200), FITC- (Sigma-Aldrich; 1:200) anti-rabbit secondary antibodies. PIN immunostaining in yeast and HeLa cells was performed as described (*13, 14*).

All preparations were observed using an epifluorescence microscope (Nikon Eclipse E600) equipped with appropriate filter sets, DIC optics, monochrome integrating CCD camera (COHU 4910, USA) or colour digital camera (DVC 1310C, USA).

Quantitative analysis of root gravitropism

5 days old seedlings of WT-Col, *pgp1pgp19*, *XVE-PIN1* and *XVE-PIN 1/pgp1pgp19* lines grown vertically were transferred on new MS plates containing 4 μM β-estradiol for 12 hours. Seedlings were then stretched and plates turned through 135° for additional 12 hour gravity stimulation in dark. The angle of root tips from the vertical plane was measured using ImageJ software (NIH, USA). All gravistimulated roots were assigned to one of the

eight 45° sectors on gravitropism diagram. The length of bars represents the percentage of seedlings showing respective direction of root growth.

Auxin accumulation assays in plant, HeLa and yeast cells

Auxin accumulation experiments in suspension-cultured tobacco BY-2 cells were performed and the integrity of labeled auxins during the assay was checked exactly as described (*15, 8, 12*). The same protocol was used for suspension-cultured *Arabidopsis* cells. Labeled [^{3}H]IAA, [^{3}H]2,4-D and [^{3}H]Trp (specific activities 20 Ci/mmol, American Radiolabeled Chemicals, St. Louis, MO), and [^{3}H]NAA (specific radioactivity 25 Ci/mmol, Institute of Experimental Botany, Prague, Czech Republic) were used. Briefly, the accumulation was measured in 0.5-mL aliquots of cell suspension. Each cell suspension was filtered, resuspended in uptake buffer (20 mM MES, 40 mM Suc, and 0.5 mM $CaSO_4$, pH adjusted to 5.7 with KOH), and equilibrated for 45 min with continuous orbital shaking. Equilibrated cells were collected by filtration, resuspended in fresh uptake buffer, and incubated on the orbital shaker for 1.5 h in darkness at 25°C. [^{3}H]NAA was added to the cell suspension to give a final concentration of 2 nM. After a timed uptake period, 0.5-mL aliquots of suspension were withdrawn and accumulation of label was terminated by rapid filtration under reduced pressure on 22-mm-diameter cellulose filters. The cell cakes and filters were transferred to scintillation vials, extracted in ethanol for 30 min, and radioactivity was determined by liquid scintillation counting (Packard Tri-Carb 2900TR scintillation counter, Packard Instrument Co., Meriden, CT). Counts were corrected for surface radioactivity by subtracting counts obtained for aliquots of cells collected immediately after the addition of [^{3}H]NAA. Counting efficiency was determined by

automatic external standardization, and counts were corrected automatically. NPA was added as required from ethanolic stock solutions to give the appropriate final concentration. The concentration dependence of auxin accumulation in response to NPA or BFA was determined after a 20-min uptake period. For wash out experiments cells were loaded with [^{3}H]NAA (2 nM) for 30 min. After quick wash out, cells were re-suspended in fresh loading buffer but without [^{3}H]NAA; cell density before and after wash out was maintained the same. Relative NAA retention was measured as a radioactivity retained inside cells at particular time points after wash out and expressed as % of total radioactivity retained inside the cells just before wash out. The accumulation of various auxins or structurally related inactive compound (Trp) after induction of PIN or PGP expression was expressed together with SEs as the percentage of the accumulation of non-induced cells at time 30 min after application of respective labelled compound. If not indicated otherwise, 24 hours treatments with dexamethasone (1 μM) or β-estradiol (1 μM) were performed. Different sensitivities of PIN7- and PGP19-dependent [^{3}H]NAA efflux to NPA treatment (10 μM, 20 min) in *GVG-PIN7* and *GVG-PGP19:HA* cells was determined as the average value from three independent experiments. In each, the accumulation of [^{3}H]NAA was measured in NPA-treated induced and non-induced cells and scored after 20 minutes of incubation. The increase in the accumulation of [^{3}H]NAA upon NPA treatment in non-induced cells was considered as 100% and all other values expressed as the percentage of this increase.

The transient vaccinia expression system was used to transfect HeLa cells with PIN1:HA, PIN2:HA, and PIN7:HA in 6-well plates. The expression was verified by RT-PCR and western blot analysis. Auxin transport assays were performed exactly as described (*16, 14*). 16-24h after transfection cells were washed and incubated 40 min at 37°C, 5% CO_2 with

[^{3}H]IAA (26 Ci/mmol, Amersham Biosciences, Piscataway, NJ), or [^{3}H]BeA (20 Ci/mmol, American Radiolabeled Chemicals, St. Louis, MO). After incubation, cells were harvested, and retained radiolabeled substrate was quantitated. Net efflux is expressed as dpm/500,000 cells divided by the amount of auxin retained by cells transformed with empty vector minus the amount of auxin retained by cells transformed with gene of interest. Thus, the PIN-dependent decrease in retention is presented as positive efflux value expressed as means (n=3) with standard deviations. Cell viability after treatment was confirmed visually and via cell counting.

For auxin accumulation and growth assays in yeast, PIN2, PIN7 or PIN2:HA were expressed in *S. cerevisiae* strains *gef1* (*13*) and JK93da or *yap1-1* (*17*). The expression was verified by western blot analysis or immunolocalization. Export of [^{3}H]IAA (specific activity 20 Ci/mmol, American Radiolabeled Chemicals, St. Louis, MO) and [^{14}C]BeA (53 mCi/mmol, Moravek Biochemicals, Brea, CA) and growth assays were performed exactly as described (*17, 14*). The effluent species was determined by thin-layer chromatography of aliquots of exported [^{3}H]IAA (Supplementary fig. S4a) and images were taken using a phosphoimager (Cyclone, Packard Instruments) and by UV detection using [^{3}H]IAA as standard. Yeast viability before and after transport experiments was ascertained by light microscopy.

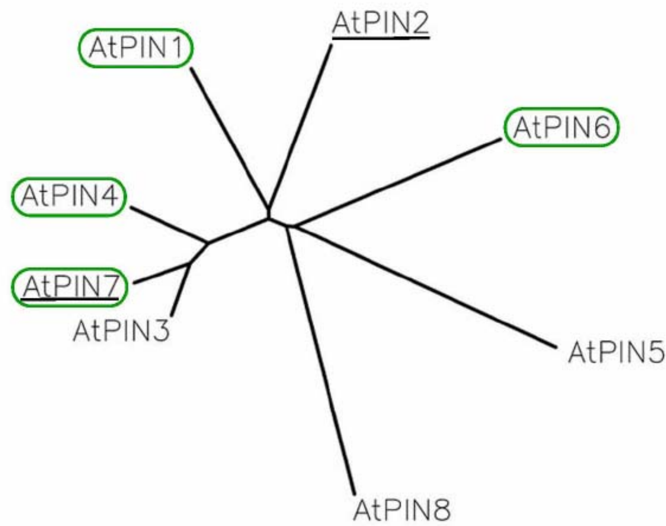

fig. S1 Arabidopsis *PIN* genes family.

Phylogenetic tree of 8 Arabidopsis *PIN* genes. Phenotypes of loss-of-function mutants in *PIN1*, *PIN2*, *PIN3*, *PIN4* and *PIN7* clearly suggest role in polar auxin transport and they all can be phenocopied by inhibitors of auxin transport (*18*). PIN6 remains functionally uncharacterized. PIN5 and PIN8 lack the middle hydrophilic domain and seem to by functionally distinct (*19*). Based on homology, *PIN7* is the most typical member of PIN family forming a distinct homologous subclade with *PIN3* and *PIN4*. *PIN6*, on the other hand, is the least homologous *PIN* from the *PIN1,2,3,4,6,7* subfamily. PIN1, PIN4, PIN6 and PIN7 (respective genes encircled in green) have been shown here to mediate auxin efflux *in planta*. PIN2 and PIN7 (genes underlined) show auxin efflux activity in heterologous systems. Notably, the confirmed expression of PIN1 in HeLa or yeast cells did not result in increased auxin efflux suggesting, in contrast to PIN2 and PIN7, that either PIN1 loses its functionality, when expressed in heterologous system, or distinctively PIN1 requires plant-specific factor(s) to mediate its function in auxin efflux.

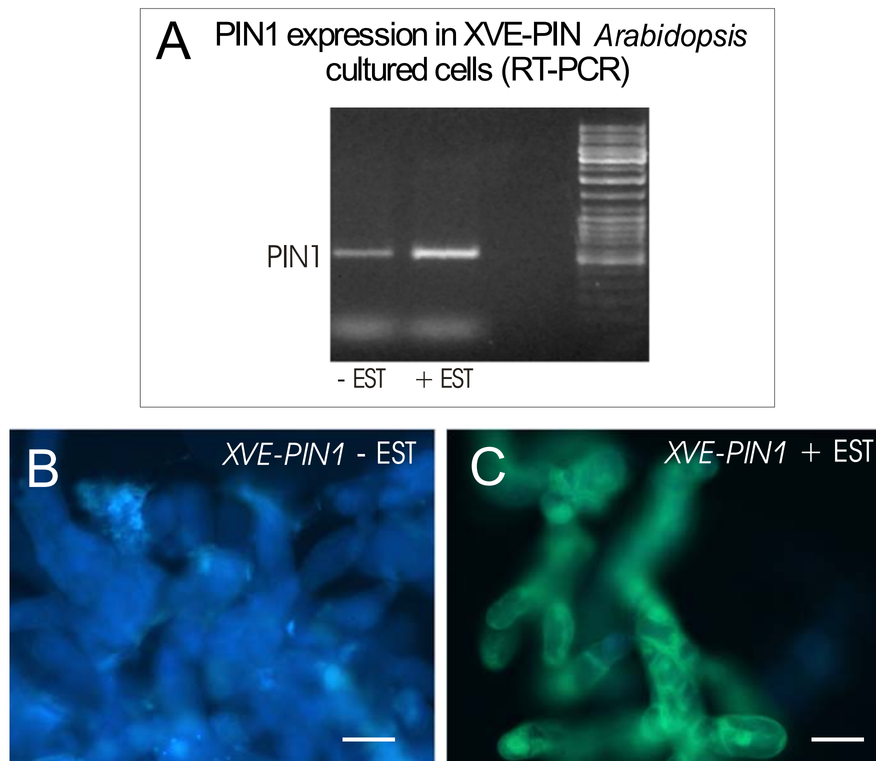

fig. S2 The expression of PIN1 in *XVE-PIN1 Arabidopsis* cultured cells

(A) RT-PCR of PIN1 in non-induced and β-estradiol-induced (1 μM, 24h) cells. (B, C) The activation of expression verified by the fluorescence of co-expressed GFP reporter. Compare the autofluorescence of cell walls in non-induced cells (B) with GFP fluorescence after 24 h incubation in 1 μM β-estradiol (C). Scale bars 30μm.

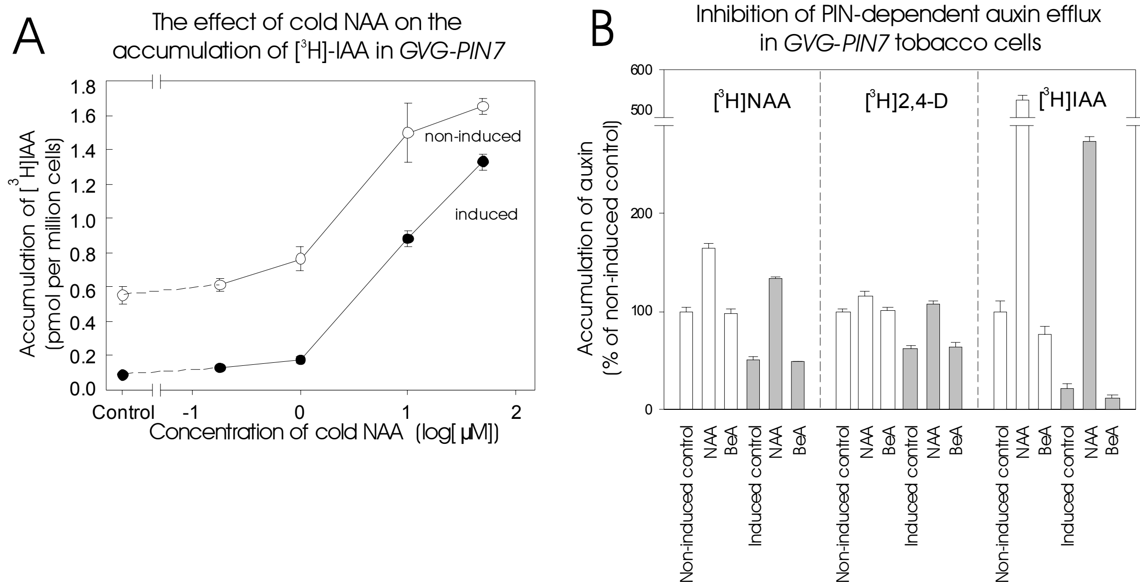

fig. S3 Auxin accumulation in *GVG-PIN7* BY-2 cells

(A) Displacement curve: The competitive inhibitory effect of cold (non-labeled) NAA on the accumulation of $[^3H]$IAA in non-induced and induced *GVG-PIN7* cells. (B) Effects of NAA and benzoic acid (BeA) on efflux of different auxins in DEX-treated (induced, full bars) and non-induced (open bars) *GVG-PIN7* cells. NAA (10 µM), a good substrate for auxin efflux machinery, interferes with both endogenous and PIN7-dependent efflux of $[^3H]$NAA, $[^3H]$2,4-D and $[^3H]$IAA in non-induced and induced *GVG-PIN7* cells, respectively. In contrast, structurally similar but inactive BeA (10 µM) does not have any detectable effect in the same experimental system.

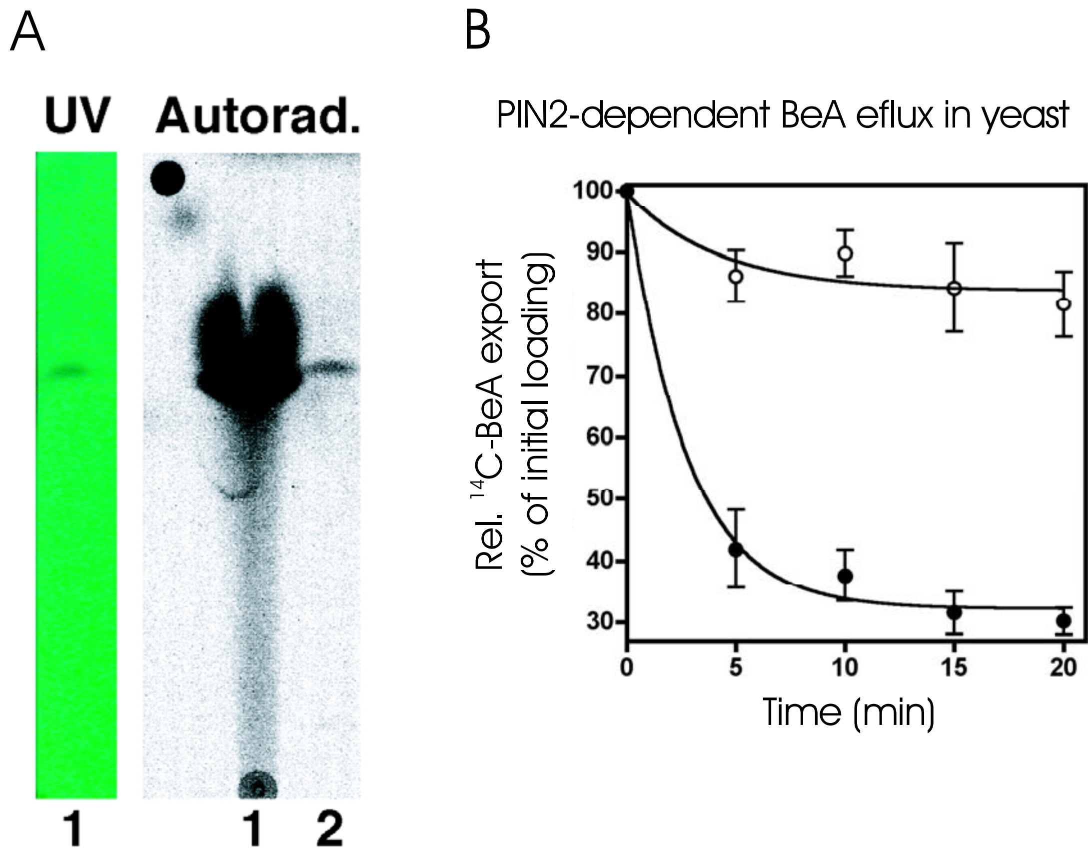

fig. S4 Control experiments for auxin efflux assays in yeast.

(A) The effluent species in yeast were determined to be [^{3}H]IAA by thin layer chromatography (lane 2). Non-exported [^{3}H]IAA was used as the standard which itself was verified by UV detection (lane 1). Images were taken using a phosphoimager (Cyclone, Packard Instruments) and by UV detection using [^{3}H]IAA as the standard. The integrity of exported [^{3}H]IAA in this assay was also proved by MS-MS, as described elsewhere (*14*).

(B) PIN2-expressing yeast show increased net efflux of [^{14}C]benzoic acid ([^{14}C]BeA)

compared to empty vector controls. [^{14}C]BeA (53 mCi/mmol, Moravek Biochemicals, Brea, CA) was used and transport experiments were performed exactly as described (*14*).

Supporting references and notes

1. E. Benková *et al.*, *Cell* **115**, 591 (2003).

2. P. J. Jensen, R. P. Hangarter, M. Estelle, *Plant. Physiol.* **116**, 455 (1998).

3. J. Zuo., Q.W. Niu, N.H. Chua, *Plant J.* **24**, 265 (2000).

4. B. Noh, A.S. Murphy, E.P. Spalding *Plant Cell* **13**, 2441 (2001).

5. T. Aoyama, N. H. Chua, *Plant J.* **11**, 605 (1997).

6. J. Mathur, C. Koncz, in *Methods in Molecular Biology: Arabidopsis Protocols*, J.M. Martinez-Zapater, J. Salinas, Eds. (Humana Press, Totowa, New Jersey, 1998), vol. 82, pp. 27-30.

7. T. Nagata, Y. Nemoto, S. Hasezawa, *Int. Rev. Cytol.* **132**, 1 (1992).

8. J. Petrášek *et al.*, *Plant Physiol.* **131**, 254 (2003).

9. A. Müller, *EMBO J.* **17**, 6903 (1998).

10. J. Friml *et al.*, *Nature* **426**, 147 (2003).

11. A. P. Smertenko *et al.*, *Plant Cell* **16**, 2035 (2004).

12. T. Paciorek *et al.*, *Nature* **435**, 1251 (2005).

13. C. Luschnig, R. A. Gaxiola, P. Grisafi, G. R. Fink *Genes Dev.* **12**, 2175 (1998).

14. M. Geisler *et al.*, *Plant J.* **44**, 179 (2005).

15. A. Delbarre, P. Muller, V. Imhoff, J. Guern *Planta* **198**, 532 (1996).

16. C. A. Hrycyna, *Biochemistry* **38**, 13887 (1999).

17. R. Prusty, P. Grisafi, G. R. Fink, *Proc. Natl. Acad. Sci. USA* **101**, 4153 (2004).

18. J. Friml, J. Wisniewska, in: *Annual Plant Reviews, Intercellular Communication in Plants,* A Fleming, Ed. (Blackwell Publishing, Oxford, UK, 2005), vol. 16, pp. 1-26.

19. I. A. Paponov, W. D. Teale, M. Trebar, I. Blilou, K. Palme, *Trends Plant Sci.* **10**, 170 (2005).